PACS numbers: 42.65.Dr; 42.65.Ky
DOI: 10.1070/QE2002v032n01ABEH002126

Temporal dynamics of parametric transformation in a Raman-active medium with the induced rotational coherence

A.V.Andreev, A.A.Valeev, V.B.Morozov, A.N.Olenin, V.G.Tunkin

***Abstract*. The collinear generation of radiation with a multicomponent spectrum is obtained upon scattering of picosecond pulses in gaseous hydrogen coherently excited by the pulsed biharmonic pump in resonance with the Raman-active rotational $S_0(1)$ transition. Probe pulses at 355 nm were almost completely transformed to the radiation with the multicomponent spectrum of width ~ 5000 cm^{-1} and the components spaced by 587 cm^{-1}. The solution of a system of equations for the four-photon Raman – parametric interaction is obtained in the plane-wave dispersionless approximation in the spectral and time representations. The equations describe the transformation of probe pulses in gas with the induced coherence into an arbitrary number of interacting spectral components. The consideration performed in the second order of the dispersion theory provides good agreement with experiments on the transformation into different spectral components depending on the probe-pulse delay.**

Keywords: *Raman-active medium, phase and frequency modulation, coherent scattering*.

1. Introduction

The Raman – parametric transformation of the laser pump by a molecular medium can be accompanied by the generation of radiation with the spectrum consisting of many lines and covering a broad region in the IR, visible, and UV ranges. This transformation has been considered in many experimental papers as an efficient method for obtaining multifrequency radiation with a spectrum consisting of equidistant or quasi-equidistant spectral lines upon vibrational and (or) rotational SRS and resonance parametric processes, in particular, in gaseous hydrogen [1 – 9].

The SRS transformation of picosecond and femtosecond pulses proceeding under substantially nonstationary conditions has a number of features. For example, the propagation of solitons can be observed upon both resonance and nonresonance SRS [10, 11]. It is interesting to use SRS and four-photon Raman – parametric processes along with self-phase modulation [12] and generation of high harmonics [13, 14] for generating femtosecond and subfemtosecond pulses [9]. Despite a great number of papers published in this field, the methods for generating this radiation and its spectral and temporal properties are not adequately studied.

In this paper, we study experimentally the generation of Stokes and anti-Stokes components upon the propagation of probe pulses in molecular hydrogen excited by the pulsed biharmonic pump resonantly with the $S_0(1)$ rotational transition. The data are analysed by considering nonstationary four-photon Raman – parametric interaction upon the propagation of probe pulses in a medium with the induced coherence.

A.V.Andreev, A.A.Valeev, V.B.Morozov, A.N.Olenin, V.G.Tunkin
Department of Physics, M.V.Lomonosov Moscow State University, Vorob'evy gory, 119899 Moscow, Russia

Received 25 June 2001
Kvantovaya Elektronika 32 (1) 54 – 58 (2002)
Translated by M.N.Sapozhnikov

2. Experimental

In the experimental setup shown in Fig. 1, we use a Nd : YAG laser emitting trains consisting of 10 – 12 30-ps pulses with a repetition rate of 1.5 Hz. Two successive electrooptical $LiTaO_3$ modulators separate the central pulse of a train, which then is amplified by a system of amplifiers. The radiation is transformed into the second harmonic in two channels and into the third harmonic in one channel. The tunable radiation is emitted by a synchronously pumped dye laser. The radiation is amplified in a dye amplifier and a single tunable peak is separated.

The 1-mJ, 532-nm second-harmonic single pulses and single 0.8-mJ, 550-nm pulses from the dye laser are used as a biharmonic pump (exciting pulses). The 0.1 mJ, 355-nm third-harmonic pulses are used as probe pulses and can be delayed with respect to the exciting pulses by the time τ, which can be varied from -0.1 to 5 ns with the help of an optical delay line. The beams of the biharmonic pump, whose polarisations are mutually orthogonal, were made coincident using a Glan prism with a side entrance, and they were combined with the probe beam on a dichroic mirror. The pump and probe beams were focused into a cell with hydrogen by a lens with the focal distance 30 cm.

The biharmonic pump tuned to the Raman resonance with the rotational 587-cm^{-1} $S_0(1)$ transition produces the coherent excitation in the medium. The probe beam scattered by this excitation is transformed to the Stokes and anti-Stokes components. The use of picosecond pulses for pumping and probing the medium allows one to neglect the dephasing directly during the interaction of radiation with the medium. By introducing the variable delay τ between pumping and probing, we can experimentally

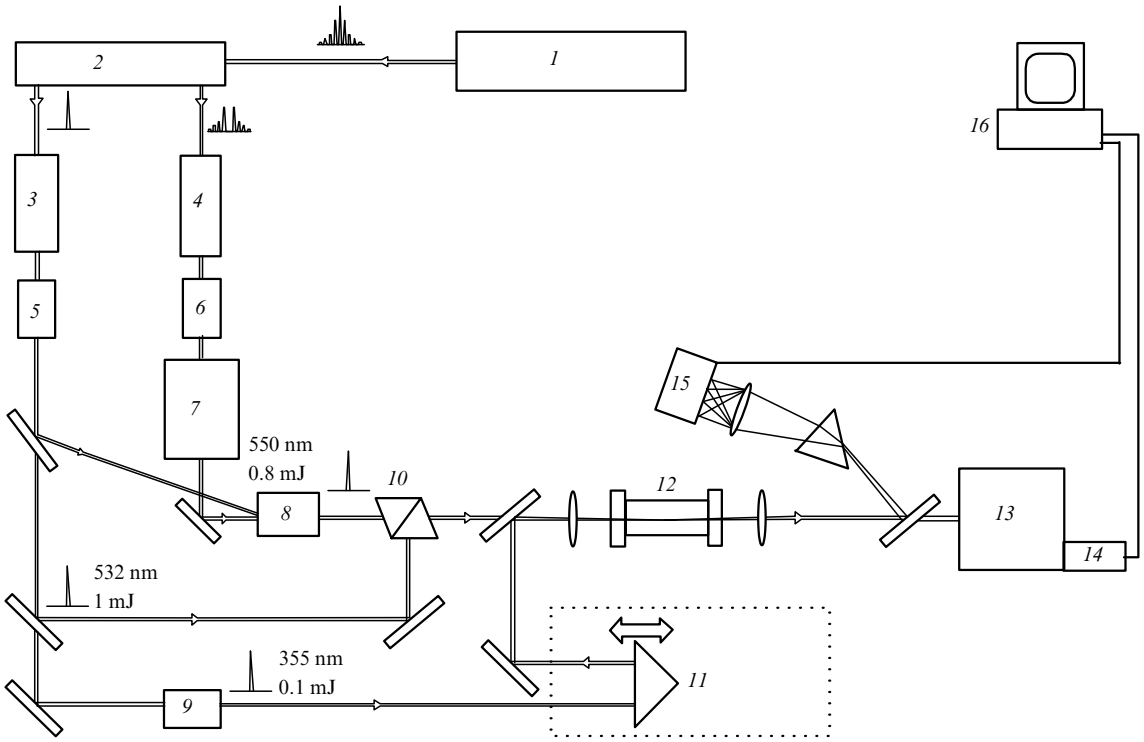

Figure 1. Scheme of the experimental setup: (*1*) Nd : YAG laser; (*2*) scheme for separating a single pulse; (*3*, *4*) Nd : YAG amplifiers; (*5*, *6*) frequency doublers; (*7*) synchronously pumped dye laser; (*8*) dye amplifier; (*9*) third-harmonic converter; (*10*) Glan prism; (*11*) delay line; (*12*) cell with hydrogen; (*13*) monochromator; (*14*) photomultiplier; (*15*) CCD camera; (*16*) computer.

determine the effect of dephasing during the time τ on the generation of a sequence of Raman lines.

Behind the cell with hydrogen, a collimating lens was placed. The radiation coming from the cell was dispersed with a 1200 lines mm^{-1} diffraction grating and detected with a CCD camera through UFS-1 and ZhS-20 light filters (not shown in Fig. 1). Fig. 2a shows the spectral components of the output radiation detected for one laser pulse at different delays of the probe pulse with respect to the pump pulses. Fig. 2b shows the relation between the energies of different spectral components for a minimal delay of the probe pulse, as well as the frequency dependence of the total transmission coefficient of the filters. To measure the dependence of the energy of individual spectral components on the delay time, they were separated with a monochromator and detected with a photomultiplier. The results of measurements are shown in Fig. 3.

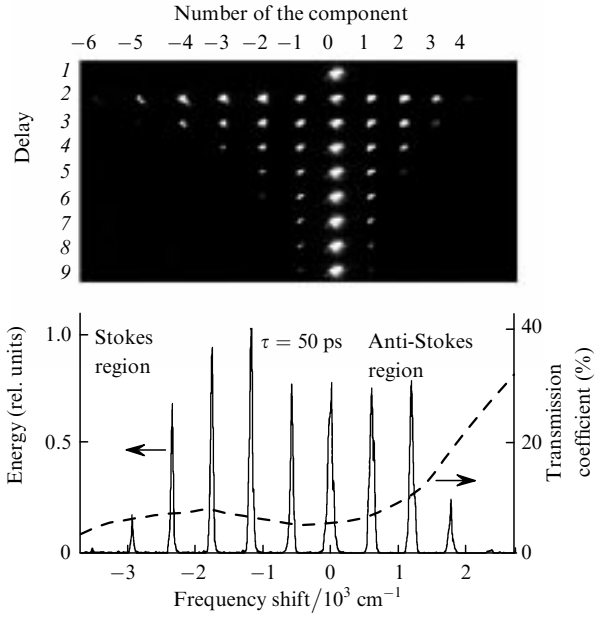

Figure 2. Spectral components of generated radiation at the exit of a cell with hydrogen for probe-pulse delays –100 (*1*), 50 (*2*), 120 (*3*), 190 (*4*), 260 (*5*), 330 (*6*), 400 (*7*), 470 (*8*) and 540 ps (9) and the hydrogen pressure 26 atm (a), as well as the relation between energies of spectral components for the 50-ps delay time and the hydrogen pressure 26 atm. The dashed curve shows the total transmission coefficient of UFS-1 and ZhS-20 light filters placed in front of the CCD camera.

3. Basic equations

Consider the equations describing the transformation of probe radiation in a Raman-active gaseous medium with induced coherence. Let the probe-wave frequency be ω_0, then frequencies of the Stokes and anti-Stokes waves will be $\omega_j = \omega_0 + j\Delta\omega$, where $\Delta\omega$ is the difference of frequencies of the biharmonic-pump waves. In this case, the strength of the total field has the form

$$E = \sum_j A_j \exp[\mathrm{i}(k_j z - \omega_j t)] + \text{c.c.}$$

where A_j are slowly varying amplitudes; z is the coordinate; $k_j = \omega_j n_j / c$ are the wave numbers of spectral components; j are the numbers of components for the Stokes ($j < 0$) and anti-Stokes ($j > 0$) regions; and n_j is the phase refractive index. The frequency interval $\Delta\omega$ between adjacent spectral components is close to the transition frequency Ω_{12}.

The system of equations for slowly varying amplitudes

of the components of an electromagnetic field in a Raman-active medium with induced coherence ($\rho_{12} = \rho_{21}^*$) has the well-known form [15]

$$\left(\frac{\partial}{\partial t} + u_j \frac{\partial}{\partial z}\right) A_j + \mathrm{i}\frac{c}{n_j} a_2 \frac{j(j-1)}{2} A_j$$

$$= \mathrm{i}2\pi\omega_j \eta_j n_j N\{[r_{11}(\omega_j, -\omega_j)\rho_{11} + r_{22}(\omega_j, -\omega_j)\rho_{22}]A_j \quad (1)$$

$$+ r_{12}(\omega_j, -\omega_{j-1})\rho_{21}A_{j-1} + r_{21}(\omega_{j+1}, -\omega_j)\rho_{12}A_{j+1}\},$$

where u_j is the group velocity; ρ_{ij} are elements of the density matrix; η_j is the group refractive index of the corresponding frequency component neglecting nonlinear effects; a_2 is the coefficient at the second-order term in the expansion of the wave vector of the radiation component in the medium in its number, which can be always written in the form

$$k_j = \frac{\omega_j n_j}{c} = a_0 + a_1 j + \frac{a_2 j(j-1)}{2} + \ldots .$$

The matrix elements $r_{11}(\omega_j, -\omega_j)$, $r_{22}(\omega_j, -\omega_j)$ and $r_{21}(\omega_{j+1}, -\omega_j)$ have the form

$$r_{11}(\omega_j, -\omega_j) = \frac{1}{\hbar}\sum_k \left(\frac{d_{1k}d_{k1}}{\Omega_{k1} - \omega_j} + \frac{d_{1k}d_{k1}}{\Omega_{k1} + \omega_j}\right),$$

$$r_{22}(\omega_j, -\omega_j) = \frac{1}{\hbar}\sum_k \left(\frac{d_{2k}d_{k2}}{\Omega_{k2} - \omega_j} + \frac{d_{2k}d_{k2}}{\Omega_{k2} + \omega_j}\right),$$

$$r_{21}(\omega_{j+1}, -\omega_j) = \frac{1}{\hbar}\sum_k \left(\frac{d_{2k}d_{k1}}{\Omega_{2k} - \omega_j} + \frac{d_{2k}d_{k1}}{\Omega_{k1} + \omega_j}\right), \quad (2)$$

$$r_{12}(\omega_{j+1}, -\omega_j) = r_{21}^*(\omega_{j+1}, -\omega_j).$$

Hereafter, we assume that the frequencies Ω_{k1} of allowed dipole transitions are much higher than the frequencies of the interacting components: $\Omega_{k1} \gg \omega_j$.

Let us write the equation for the statistically averaged nondiagonal element of the density matrix ρ (hereafter, $\rho \equiv \rho_{21}$)

$$\frac{\partial\rho}{\partial t} + \rho(\gamma + \mathrm{i}\delta + \mathrm{i}\Delta_{21}) = -\frac{\mathrm{i}}{\hbar} R \sum_j r_{21} A_j A_{j-1}^*, \quad (3)$$

where $\Delta_{21} \approx \Theta \sum_j |A_j|^2$ is the Stark shift of the frequency; Θ is the proportionality coefficient; γ is the transverse relaxation rate; and $\delta = \Omega_{21} - \Delta\omega$ is the frequency detuning.

The equation for the averaged difference of populations of the upper and lower levels ($R = \rho_{22} - \rho_{11}$) has the form

$$\frac{\partial R}{\partial t} + \frac{R - R_0}{T_1} = -\frac{2\mathrm{i}}{\hbar}\left(\sum_k r_{12} A_k^* A_{k-1}\rho_{21} - \mathrm{c.c.}\right). \quad (4)$$

Assuming that r_{11}, r_{22}, and r_{12} are independent of j, neglecting the dispersion in equation (1) ($a_2 = 0$, $u_j = u$, $\eta_j = \eta$, $n_j = n$), by introducing the current time $t_s = (t - z/u)$, and passing to new amplitudes $A'_j = A_j \exp[-2\pi\mathrm{i}\omega_0\eta n N(r_{11}\rho_{11} + r_{22}\rho_{22})t]$, we write (1) in terms of time t and current time t_s:

$$\left.\frac{\partial}{\partial t}\right|_{t_s=\mathrm{const}} A'_j = \mathrm{i}2\pi\omega_0\eta n N\left(r_{12}\rho A'_{j-1} + r_{21}\rho^* A'_{j+1}\right). \quad (5)$$

We assume that coherent excitation of the medium is the same over its entire length, i.e., ρ is independent of t for $t_s = \mathrm{const}$. In this case, the system of differential equations (5) is linear, with constant coefficients, and represents recurrence relations for Bessel functions.

At the entrance to the medium $z = 0$ ($t = t_s$), the probe-wave amplitude A'_0 is specified. By passing to old amplitudes A_j and coordinates t, z, we obtain

$$A_j(t, z) = A_0\left(t - \frac{z}{u}, 0\right) J_j\left(2|\xi|\frac{z}{u}\right) \exp\left[\mathrm{i}\left(j\arg\xi + \frac{\psi z}{u}\right)\right]. \quad (6)$$

Here, $\xi = \mathrm{i}2\pi\omega_0\eta n N r_{12}\rho$; $\arg\xi$ is the complex argument of ξ; $\psi = 2\pi\mathrm{i}\omega_0\eta n N(r_{11}\rho_{11} + r_{22}\rho_{22})$; J_j is the Bessel function of the order j. In this case, the total field has the form

$$E(t, z) = E_0\left(t - \frac{z}{u}, 0\right)$$

$$\times \exp\left\{\mathrm{i}\frac{z}{u}\left[2|\xi|\sin\left[-\Delta\omega\left(t_s + \frac{u - v}{uv}z\right) + \arg\xi\right] + \psi\right]\right\} \quad (7)$$

$$+ \mathrm{c.c.}$$

Here, v is the phase velocity in the medium. It follows from this that during the Raman–parametric transformation of the probe pulse in the dispersionless model in the approximation of plane waves and linear unidirectional polarisation, the phase modulation of radiation occurs at the coherently excited transition described by equation (7).

4. Discussion of results

The choice of the Raman-active $S_0(1)$ rotational transition ($\Omega_{21} = 587\ \mathrm{cm}^{-1}$) of hydrogen for the study provides the fulfilment of the phase-matching condition for generation of several first Stokes and anti-Stokes components at relatively high pressures. The expansion coefficients a_j of the wave vector of the order higher than first, which determine the phase mismatch, are specified by the frequency dependence of the refractive index. The refractive index of gases far from the absorption line is well described by the dispersion Cauchy formula [16] $n - 1 = A(1 + B/\lambda^2)$. Here, λ is the wavelength of light and A and B are constants. For hydrogen under normal conditions, $A = 13.6 \times 10^{-5}$ and $B = 7.7 \times 10^{-11}\ \mathrm{cm}^2$. From this, we can find the phase mismatch a_2

$$a_2 = \frac{\partial^2 k}{\partial\omega^2}\Delta\omega^2 = \frac{3}{2}AB\frac{\omega\Delta\omega^2}{\pi^2 c^3} = p0.0027\ \mathrm{cm}^{-1}\ \mathrm{atm}^{-1}.$$

For maintaining phase matching during the propagation of radiation components, the phase incursion between these components should be lower than π. This condition can be written in the form

$$\frac{a_2 j_{\max}^2}{2} L < \pi$$

where L is the length of the medium. For $L = 3$ cm, $j_{\max} = 4$, and $p_{\max} = 26$ atm, the phase-matching condition is still fulfilled.

The biharmonic pump allows us to excite selectively the chosen Raman-active transition without the threshold. In this case, no negative effects of the self-action or distortion of the spatial profile of beams are present, which can be observed upon powerful one-frequency pumping. During the propagation of pump pulses entering the medium at the moment $t = 0$, a coherence wave is produced in the medium, whose amplitude decays exponentially (by neglecting an inhomogeneous broadening):

$$\rho = \rho_0 \theta\Big(t - \frac{z}{u}\Big) \exp\Big[-\gamma\Big(t - \frac{z}{u}\Big)\Big].$$

Here, ρ_0 is the maximum coherence amplitude; $\theta = 0$ and 1 for negative and nonnegative arguments, respectively.

Once the probe pulse propagated through the medium of length z (the delay time of the probe pulse is $\tau = t - z/u$), the frequency components with amplitudes

$$A_j = A_0(z=0) J_j\left[\frac{2|\xi_0|\theta(\tau) z \exp(-\gamma\tau)}{u}\right] \exp\left[\mathrm{i}\left(j \arg \xi + \frac{\psi z}{u}\right)\right] \tag{8}$$

will be observed.

For small z, the amplitudes of the anti-Stokes and Stokes components ($j = \pm 1$) linearly depend on the induced coherence. For sufficiently large values of z, the higher-order Stokes and anti-Stokes components appear. A great difference between the probe-pulse frequency and frequencies of pump pulses in our case allows us to separate spectral components generated upon scattering of the probe pulse from components generated upon scattering of pump pulses. A comparison of the energies of components generated at small delay (Fig. 2b) shows that the initial probe beam is almost completely transformed to radiation with a multicomponent spectrum. As the delay time is increased, the conversion efficiency decreases because of the destruction of coherence of the ensemble due to dephasing. For a pressure of 26 atm, the dephasing time is $T_2 = 130$ ps, which is several times higher than the duration of the pump and probe pulses.

Fig. 3 shows the experimental dependences of energy of the first three Stokes and anti-Stokes components on the delay time, as well as the change in the probe-beam energy. The higher-order spectral components are characterised by a faster decay, and the number of generated spectral components decreases with the delay time. The location of the curves in Fig. 3 along the vertical axis is arbitrary and was chosen for the convenience of their representation.

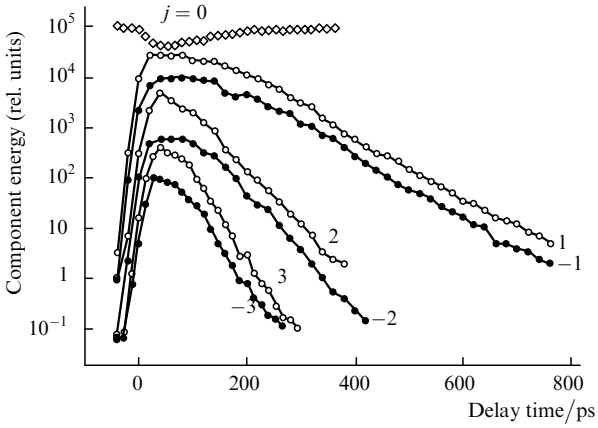

Figure 3. Experimental dependences of the energy of the probe beam ($j = 0$), the first three Stokes ($j = -1, -2, -3$) and anti-Stokes ($j = 1, 2, 3$) components on the probe-pulse delay time for the hydrogen pressure 26 atm.

The true relation between energies of the spectral components is shown in Fig. 2b. The time dependences of energies of the spectral components calculated by expression (8) taking the probe-pulse duration into account, which are presented in Fig. 4a, are in qualitative agreement with the experiment. The best agreement with the experiment is achieved by taking into account the second-order dispersion ($\partial^2 k/\partial\omega^2 = 8 \times 10^{-30}$ s^2 cm^{-1} [16]) by solving numerically the system of equations (1), (3) for $a_2 \neq 0$.

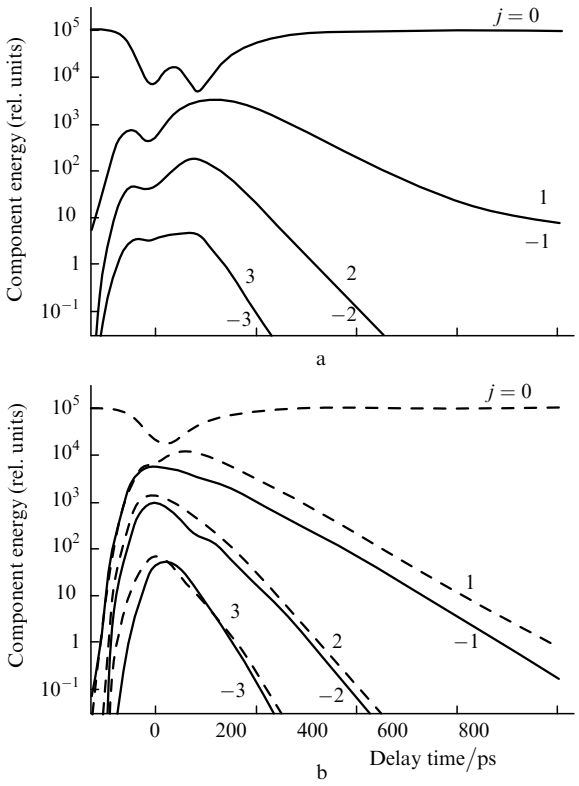

Figure 4. Dependences of the energy of spectral components on the probe-pulse delay time calculated from (8) (a) and taking into account the second-order dispersion (b) for the hydrogen pressure 26 atm: probe beam ($j = 0$), the first three Stokes ($j = -1, -2, -3$) and anti-Stokes ($j = 1, 2, 3$) components.

The result of the corresponding calculations is shown in Fig. 4b. Due to the deviation from phase matching, the number of generated spectral components does not increase infinitely. Fig. 5 shows the results of calculations of the propagation dynamics of the probe wave and the first three anti-Stokes components performed in the plane-wave approximation by neglecting phase matching or taking it into account. In the first case, the total intensity of these components gradually decreases due to energy transfer to higher-order spectral components. In the second case, the energy is gradually redistributed among the first several spectral components.

In the plane-wave approximation, an increase in time is in fact equivalent to an increase in pressure. We observe no

infinite increase in the number of spectral components with increasing pressure up to 26 atm in our experiments. It follows from Fig. 5 that the probe-wave energy should almost completely transfer to higher-order components at a certain propagation length. We did not observe this in our experiments, and the probe-wave intensity at the exit from the medium only slightly differed from that of the adjacent components. It can be explained by focusing, which complicates the transformation process. A better agreement with the plane-wave approximation can be achieved by increasing the length of the medium and using a long-focus lens.

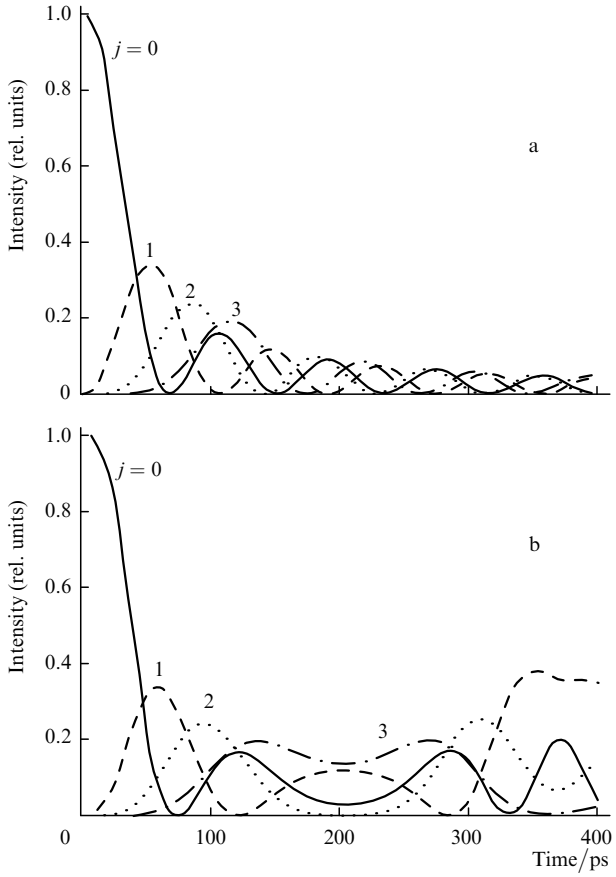

Figure 5. Dependences of the energy of spectral components on the propagation time calculated from (8) (a) and taking into account the second-order dispersion (b): probe beam ($j = 0$) and the first three anti-Stokes components ($j = 1, 2, 3$).

5. Conclusions

We have observed the collinear generation of a number of Stokes and anti-Stokes components with the spectrum of width ~ 5000 cm^{-1} and the spacing between the components equal to 587 cm^{-1} upon scattering picosecond pulses in gaseous hydrogen coherently excited by the pulsed biharmonic pump in resonance with the rotational $S_0(0)$ transition. The theoretical model has been developed in the plane-wave dispersionless approximation, which describes the transformation of probe pulses propagating in a Raman-active medium with the induced coherence into anti-Stokes and Stokes components.

Acknowledgements. This work was supported by the Russian Foundation for Basic Research (Grants Nos 99-02016093 and 01-02-16044).

References

1. Morozov V.B., Tunkin V.G., Olenin A.N. *Zh. Eksp. Teor. Fiz.*, **115**, 479 (1999).
2. Bespalov V.G., Krylov V.N., Mikhailov V.N., Parfenov V.A., Stasel'ko D.I. *Opt. Spektrosk.*, **70**, 332 (1991).
3. Drabovich K.N., Klyukach I.L., Orlov R.Yu., Skidan I.B., Telegin L.S. *Scientific Proceedings of Kazan State Pedagogical Institute* (Kazan, 1973) No. 125, p. 93.
4. Wilke V., Schmidt W. *Appl. Phys.*, **18**, 177 (1979).
5. Jarvis G.B., Mathew S., Kenny J.E. *Appl. Opt.*, **33**, 4938 (1994).
6. Baldwin K.G.H., Harangos J.P., Burgess D.D. *Opt. Commun.*, **52**, 351 (1985).
7. Grasyuk A.Z., Zubarev I.G., Kotov A.V., Mikhailov S.I., Smirnov V.G. *Kvantovaya Elektron.*, **3**, 1062 (1976) [*Sov. J. Quantum Electron.*, **6**, 568 (1976)].
8. Sokolov A.V., Walker D.R., Yavuz D.D., Yin G.Y., Harris S.E. *Phys. Rev. Lett.*, **85**, 562 (2000).
9. Wittmann M., Nazarkin A., Korn. G. *Phys. Rev. Lett.*, **84**, 5508 (2000).
10. Andreev A.V. *Zh. Eksp. Teor. Fiz.*, **86**, 412 (1998).
11. Kaplan. A.E. *Phys. Rev. Lett.*, **73**, 1243 (1994).
12. Fork R.L., Brito Cruz C.H., Becker P.C., Shank C.V. *Opt. Lett.*, **12**, 483 (1987).
13. Platonenko V.T., Strelkov V.V. *J. Opt. Soc. Am. B*, **16**, 435 (1999).
14. Platonenko V.T., Strelkov V.V. *Kvantovaya Elektron.*, **24**, 799 (1997) [*Quantum Electron.*, **27**, 779 (1997)].
15. Shen Y.R. *The Principles of Nonlinear Optics* (New York: Plenum, 1984; Moscow: Nauka, 1989).
16. Akhmanov S.A., Nikitin S.Yu. *Fizicheskaya optika* (Physical Optics) (Moscow: Izd. Moscow State University, 1998).